Design and Application of a Magnetic Bearing for Vibration Control and Stabilization of a Flexible Rotor

C.R. BURROWS*, N. SAHINKAYA*, A. TRAXLER+, G. SCHWEITZER+

* School of Mechanical Engineeering, University of Bath, U.K.
+ ETH Zurich, Switzerland

Abstract

This paper describes the design of a magnetic actuator designed to control the synchronous vibration of a 2.3m long 100mm diameter rotor supported on oil-film bearings. An algorithm is described which allows the control force to be computed to minimise the synchronous rotor vibration without prior knowledge of oil-film or rotor characteristics nor of the inherent out-of-balance distribution along the rotor. In this approach the magnetic actuator is first used to apply sequential test signals along two orthogonal axes whilst the shaft is rotating. The corresponding displacements are measured and the algorithm used to determine the control forces to be applied by the actuator. The process is applied sequentially as the rotor is run-up from rest to the required operating speed. Some experimental results are presented to demonstrate the ability of this technique to significantly reduce the synchronous vibration. It is also discussed how the electromagnetic actuator can be used to avoid the instability associated with oil-whirl.

1. Actuator design

Electromagnetic actuators can be used to apply forces to a rotor without contact. These forces may be controlled by an independent external source, or by the rotor vibration. Thus the actuators can be used as a contactless excitation device e.g. for parameter estimation studies, as an active damper, or as an active bearing.

Magnetic actuators can be designed for quite different applications[1]. The objectives of this design are small overall dimensions of the actuator, high force output over a wide frequency range, and inherent capability for the dynamic requirements of vibration control.

Fig. 1 shows the electromagnetic actuator. It consists mainly of a magnet unit (a), power amplifiers with some additional electronic network (b), a rotor sleeve (c) and sensors (d). The inner diameter of the actuator is 190 mm, the gap between rotor sleeve and actuator is 1.0 mm, the length including a gap limiting roller bearing is 150 mm and the maximum force is 1200 N. The displacement sensors are of the eddy-current type. They have a measurement range of two millimetres and measure signals up to 10 kHz. Due to the direct measurement of displacements, the controllability of the displacements in the subsequent vibration control will be optimal.

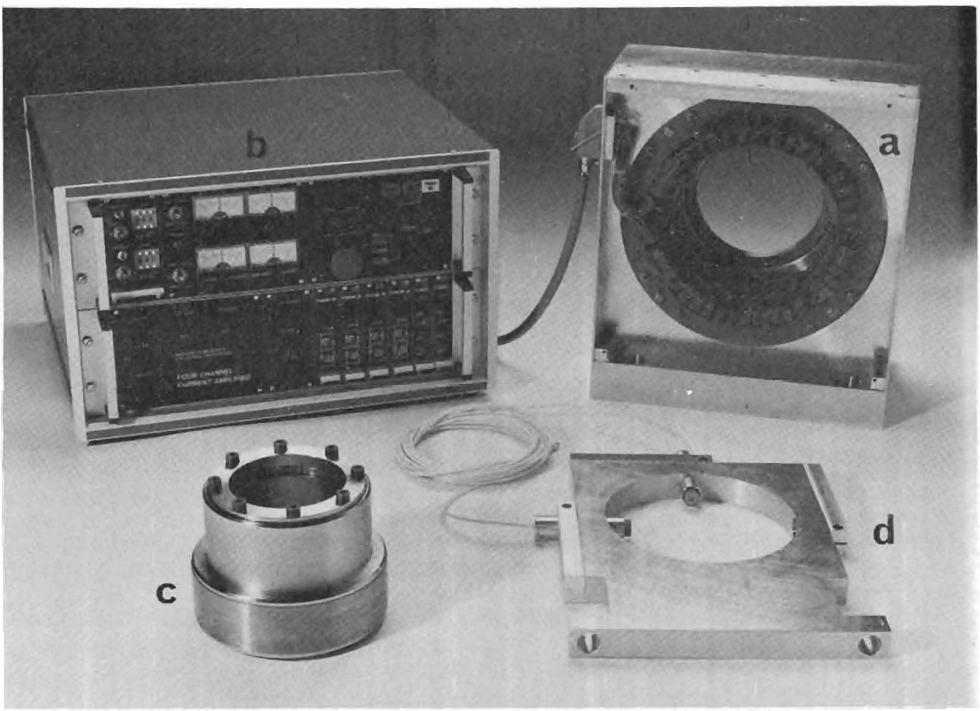

Fig. 1: Magnetic Actuator ETH-190/50/1
a) Magnet unit b) Power amplifier and signal conditioning c) Rotor sleeve d) Sensor unit.

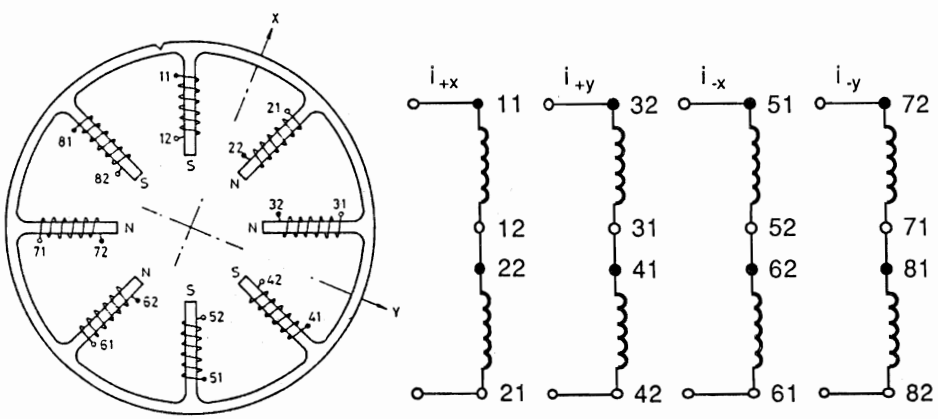

Fig. 2: a) Magnet configuration of the actuator b) Connection-diagram of the coils

The magnet configuration of the actuator is shown in Fig. 2a. The magnet has eight poles, carrying coils. The configuration corresponds to four U-shaped magnets and therefore the coils of each pole-pair are connected together as shown in Fig. 2b. Each pole-pair is energized by one of four power amplifier-channels. The number of coils and amplifiers could be minimized down to three[2], but the magnet configuration with eight poles needs smaller coil-heads and thus less space. And the eight-pole design with its inherent decoupling of the x and the y-axis simplifies the control, and makes it faster.

One of the objectives of the design of an electromagnetic actuator is to make optimum use of the available space to maximise the attainable control force. This is achieved by judicious alocation of the space between that needed by the iron core and that for the windings. The optimisation process has been done with the help of a CAD program.

2. Actuator control

The actuator is designed to give linear input/output characteristics, that is the generated forces are proportional to the input signals to the power amplifiers. This simplifies design of the control system for the vibration control at the expense of slightly more complex hardware. This can be justified on the basis that there is a large body of knowledge to aid with the design of linear control systems but the design of nonlinear systems is still less well-defined. The problem is magnified because of the complexity of the equations needed to model a flexible rotor, especially if it is carried on oil-film bearings which introduce co-ordinate coupling[3].

The nonlinear characteristics of the magnets are linearized, using bias currents and differential currents in corresponding pairs of magnets [1]. An electronic circuit calculates for the two corresponding power amplifiers of the x and the y direction the output currents i+ and i- from the force control signal U_f.

$$i_{+x} = k\,(U_o + U_{fx}); \quad i_{+y} = k\,(U_o + U_{fy}) \tag{1}$$

$$i_{-x} = k\,(U_o - U_{fx}); \quad i_{-y} = k\,(U_o - U_{fy}) \tag{2}$$

Usually, the bias signal U_o is equal to the maximum of the force control signal U_f. Neglecting saturation effects and leakage flux, the generated forces F_x and F_y are proportional to the force control signal U_{fx} and U_{fy}. They depend significantly on the position of the rotor within the magnet unit. Furthermore this linearization method leads to the desired linear force-displacement characteristics of the actuator[1]. The linearized input-output relation of the actuator can be expressed by

$$F_x = k_i\,U_{fx} + k_s\,x \tag{3}$$

$$F_y = k_i\,U_{fy} + k_s\,y \tag{4}$$

where k_i and k_s are hardware dependend constants and x and y are the displacements of the rotor from its zero-position within the magnet. Fig. 3 shows the measured force characteristics of the actuator.

For vibration control the actuator forces should be controllable in a large frequency range.

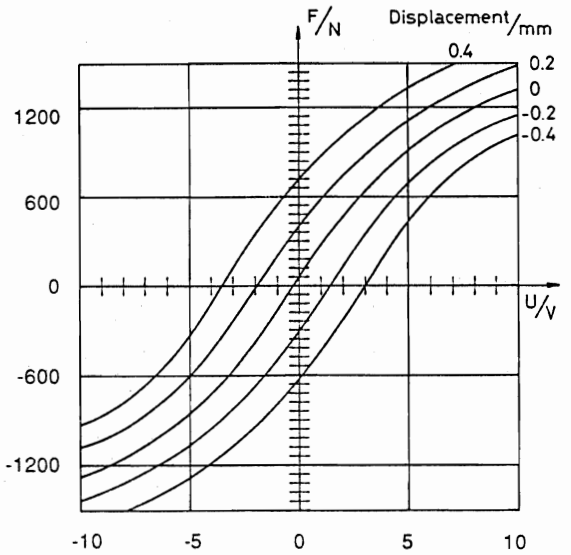

Fig. 3: Measured force characteristics of the actuator.

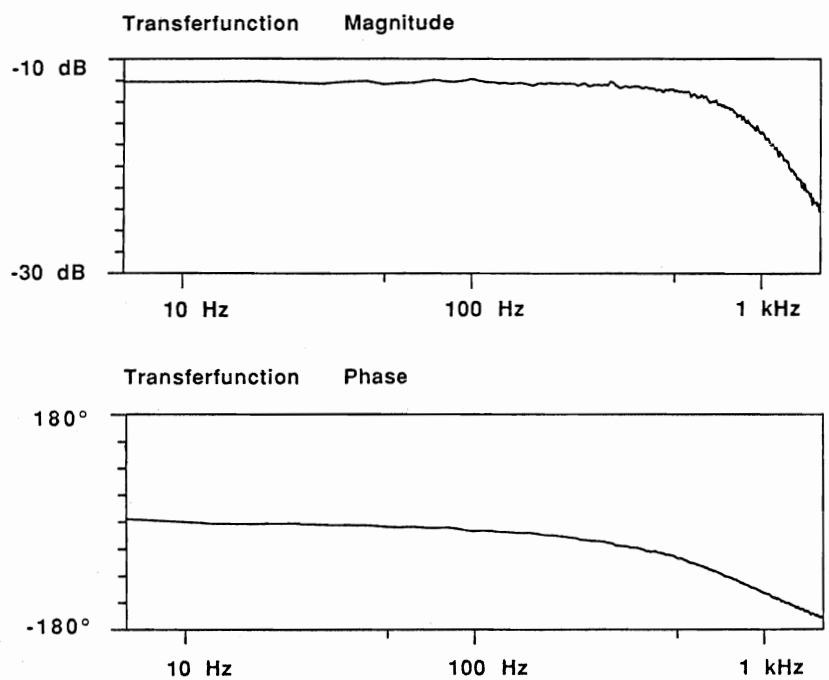

Fig. 4: Measured transfer function: Force output of the actuator / Input signal.

The amplitude of the forces will be limited by the current and the voltage that can be supplied by the power amplifiers. In simple terms: the higher the maximum current output, the higher the attainable force amplitude, and the higher the maximum voltage, the higher the maximum frequency at which this maximum force amplitude can be achieved.

To keep the losses low, the power amplifiers are of a chopper type. They work with pulse-width-modulation at a pulse frequency of 50 kHz. The applied voltage is 310 V and the maximum current of each channel is 2.8 A. With this power, the maximum force amplitude of 1200 N can be applied up to 24 Hz. At frequencies higher than 24 Hz, the maximum force amplitude reduces 20 dB per decade, i.e. the maximum force amplitude at 240 Hz is 120N.

The small signal performance of the actuator is given by the linear transfer function of the electromagnet-power amplifier combination[2]. The measured transfer function is shown in Fig. 4.

3. Rig.

The actuator described above was applied to a 2.3m long 100m diameter steel rotor carried on two oil-film film bearings. These bearings cause coupling between axes [3] as well as introducing the possibility of instability due to oil-whirl. It has been shown elsewhere that the actuator can stabilise the system in addition to reducing the synchronous vibration [4]. The arrangement is shown in Fig. 5 from which it is clear that the rotor carried two large overhanging discs of mass 93kg. each.

The rotor was driven by a 25kW d.c. variable speed motor over a speed range of 0-5000 rev/min.

The journal bearings had a 10 mm circumferential central groove and 35 mm land along either side. The measured diametral clearance was between 0.305 mm and 0.279 mm. The static load per land was 828 N. Shell Tellus oil T15 (average viscosity 0.013 Nsm^{-2} at the average operating temperature) was gravity fed to the grooves from a 180 litre reservoir. No end seals were employed.

Shaft vibration was monitored by eight eddy current proximity probes. The signals were conditioned before being fed to an ADC. The computed control forces were fed back to the actuator through a DAC. These convertors were synchronised by two signals (one pulse/rev and 36 pulse/rev) generated by optical switches actuated by a slotted disc mounted on the drive shaft.

4. Vibration Control Algorithm

The rotor-bearing system can be modelled as a multimass linear system. If $\underline{q}$ represents the complex displacement vector for the measured stations, then the synchronous response to a change $\delta\underline{u}(jw)$ in the control vector $\underline{u}(jw) = (u_x\ u_y)^T$ can be formulated as follows:

$$\underline{q} = \underline{q}_0 - (\underline{R}_x, \underline{R}_y)\,\delta\underline{u} = \underline{q} - \underline{R}\,\delta\underline{u} \qquad (5)$$

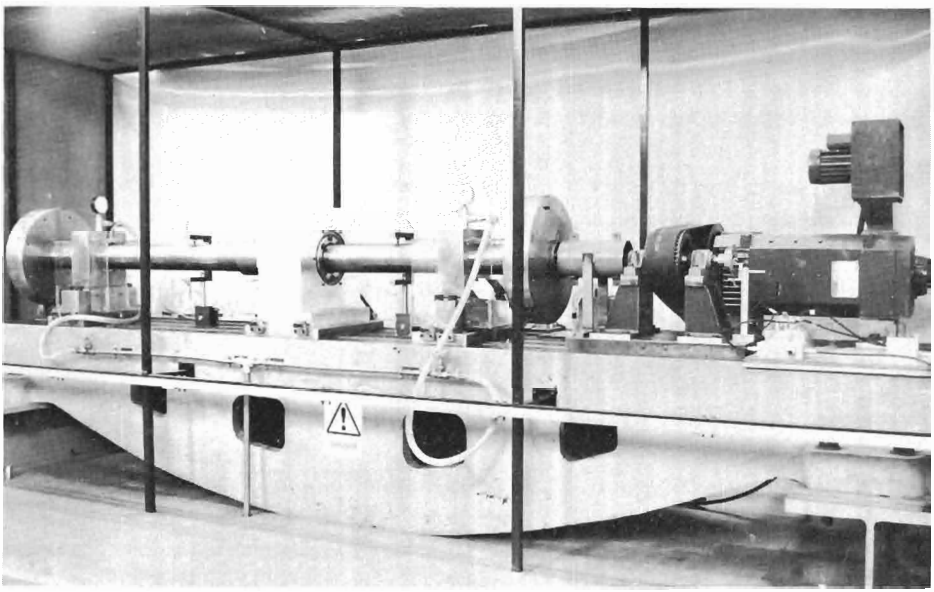

Fig. 5: Test Rig

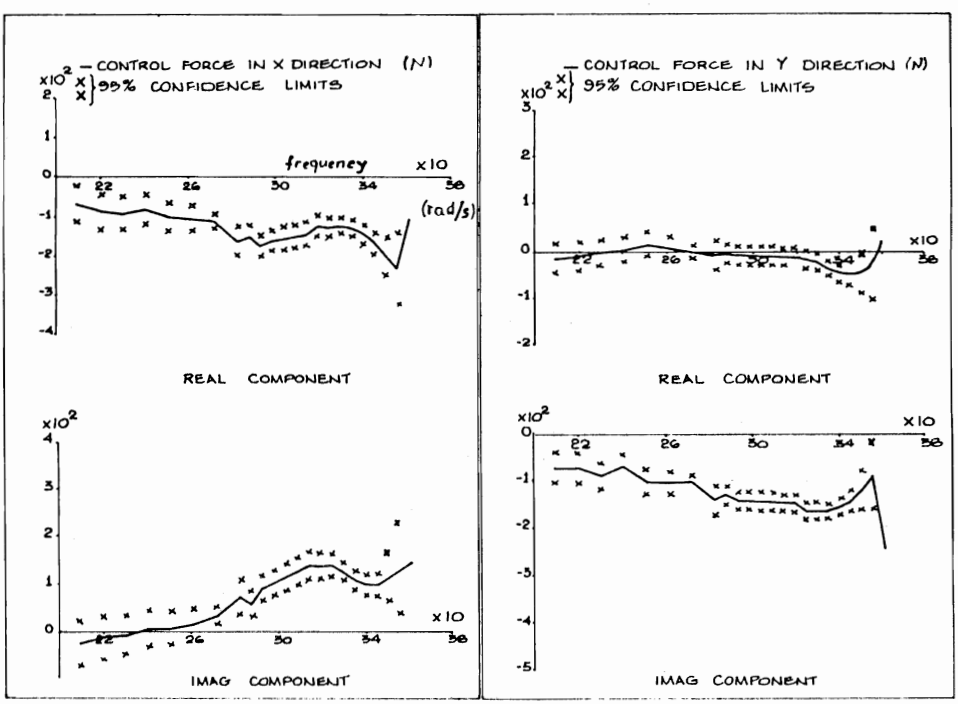

Fig. 6: Control forces calculated on-line

The complex scalars u_x, u_y are the control forces along x and y axes.The change $\delta\underline{u}$ is not constrained to be a small *variation* providing conditions for linearity are not violated. The corresponding complex vectors of influence coefficients are $\underline{R}_x$, $\underline{R}_y$. The displacement vector is $\underline{q}_o$.

Equation (5) can be rewritten as follows

$$\underline{q}_o = (\underline{R}_x, \underline{R}_y)\, \delta\underline{u} + \underline{q} \qquad (6)$$

Then, the Least Square estimation of $\delta\underline{u}$ to minimize the performance index $(\underline{q}^T\underline{q})$ is as follows

$$\widehat{\delta\underline{u}} = (\overline{\underline{R}}^T \underline{R})^{-1} \overline{\underline{R}}^T \underline{q}_o \qquad (7)$$

where $(\overline{\underline{R}})$ represents the complex conjugate, and T denotes the transpose. The above optimum force expression depends on the measured response and the corresponding influence coefficients of the system. The difficulty of assigning reliable theoretical values to the elements of $\underline{R}(jw)$ associated with the oil-film bearing coefficients is well known. This problem is overcome by estimating the $\underline{R}$ matrix on-line.

The overall control is achieved by the help of a digital computer. Pulses are generated once and 36 times per revolution to synchronise the input(displacement) and output(force) to and from the computer. The overall control algorithm can be summarised as follows

(i) sample displacements and perform FFT to construct $\underline{q}_o$ (jw)

(ii) set $\delta\underline{u} = \begin{pmatrix} 0.1\, u_x \\ 0 \end{pmatrix}$, sample displacements and perform an FFT to construct $\underline{q}_{o,1}$ (jw) and calculate $\underline{R}_x$ as follows

$$\underline{R}_x = (\underline{q}_{o,1} - \underline{q}_o)/(0.1\, u_x)$$

(iii) set $\delta\underline{u} = \begin{pmatrix} 0 \\ 0.1\, u_y \end{pmatrix}$, sample displacements and perform an FFT to construct $\underline{q}_{o,2}$(jw) and estimate $\underline{R}_y$ as follows

$$\underline{R}_y = (\underline{q}_{o,2} - \underline{q}_o)/(0.1\, u_y)$$

(iv) estimate optimum control force adjustments from equation (7)

(v) check the statistical data on $\widehat{\delta\underline{u}}$ (goodness of fit and standard deviation) to assess its validity.

If not suitable set $\delta\underline{u} = \begin{pmatrix} 0 \\ 0 \end{pmatrix}$ and go to (i)

If suitable set $\delta\underline{u} = \widehat{\delta\underline{u}}$

(vi) monitor speed and displacements. Whenever updating is required go to (i)

It is important to note that a background program ensures that the synchronous control forces are continuously fed to the magnetic actuator independent of the speed of the above control algorithm. (i.e. the previous value of $\underline{u}$ is retained until a change is required). Initially, typically at low speed, $\delta\underline{u}$ in (ii) and (iii) is set at an arbitrary value. This is updated

after the first implementation of the above algorithm. Since the force is applied in open loop there is no danger of causing instability. The statistical data obtained from the Least Square estimator is discussed in detail in Reference [3].

5. Results

The actuator is able to apply forces along the horizontal and vertical axes. The control algorithm determines the correct amplitude and phase of each force to minimise the performance index. It is stressed that this is done without knowledge of the bearing and rotor parameters nor of the unbalance distribution. Some typical optimum control forces obtained experimentally are shown in Fig. 6. This figure also includes confidence bounds generated by the algorithm. The corresponding controlled synchronous response is compared with the uncontrolled response in Figure 7. This shows the amplitude response at two different sections along the rotor. The significant reduction in vibration due to the magnetic actuator is apparent. The results are obtained by use of horizontal and vertical displacement measurements at three rotor stations. The consumed power by the magnetic actuator to provide the reduction in amplitude was typically 250W. It is significant to note that unlike many results presented in the literature, the controlled response is compared with the damped response of the rotor and not the undamped vibration. There is a ninety per cent reduction in amplitude at the critical speed. It has been shown also [5] that the reduction in synchronous response could not be achieved using *local* closed-loop control because that would require negative stiffness and damping values which would lead to instability.

Although oil-whirl did not occur it can be shown that feedback can be used to increase the stable operating range(before minimising the synchronous vibration). This leads to the idea of combined open loop and closed loop control using one actuator to both improve stability and reduce vibration.

6. Conclusions

The paper describes the design of a magnetic actuator for use with a 100 mm diameter and 2.3 m long rotor suported on oil-film bearings. A control algorithm has been implemented for in-situ tuning of the magnetic actuator to reduce synchronous vibration. The control has been achieved without prior knowledge of any system parameters or unbalance distribution. This is particularly significant because oil-film bearing parameters cannot be accurately predicted from theoretical modelling.

The approach described here allows automatic on-line tuning of the actuator to the system. Monitoring the actuator signals provides a facility for condition monitoring to detect changes in system characteristics associated with the rotor or bearings.

Acknowledgements

The results presented here were obtained by Dr. S Clements, as part of his Doctoral Studies in the University of Strathclyde, under supervision of C R Burrows and M N Sahinkaya. This work was supported by SERC.

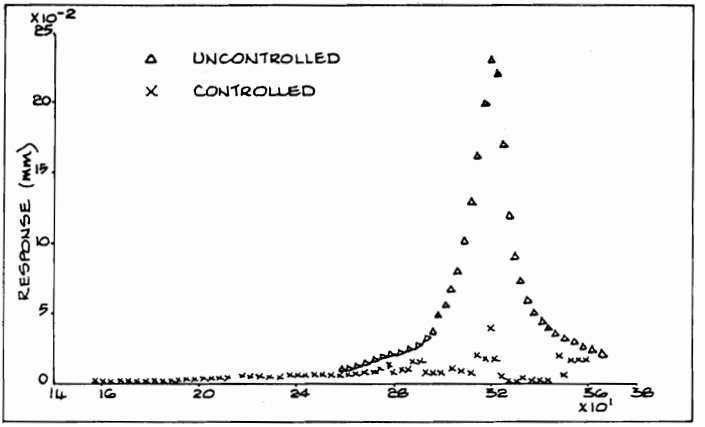

Fig. 7: a) Response at the rotor station (a)

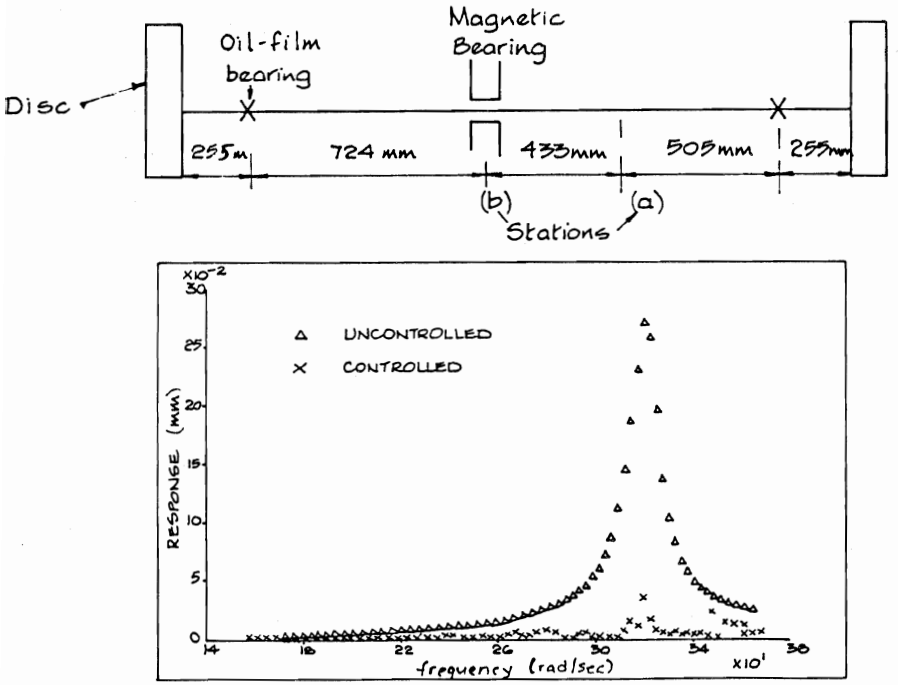

Fig. 7: b) Response at the rotor station (b)

References

1. SCHWEITZER, G & TRAXLER, A.
Design of Magnetic Bearings,
International Symposium on Design and Synthesis, The Japanese Society of Precision Engineers, Tokyo, July 1984.

2. BRADFIELD, C D, ROBERTS J B & KARUNENDIRAN, P.
Performance of an electromagnetic bearing for the vibration control of a supercritical shaft. Proc. Instn. Mech. Engrs., Vol. 201, NoC3, I MechE, 1987.

3. BURROWS, C R & SAHINKAYA, M N.
Vibration control of multi-mode rotor-bearing systems, Proc. Royal Soc., Lon. A386, 1983, p77-94.

4. SAHINKAYA, M N & BURROWS, C R.
Control of stability and the synchronous vibration of a flexible rotor supported on oil-film bearings, Trans. ASME, JDSMC, Vol. 107, 1985, p139-144.

5. BURROWS, C R & SAHINKAYA, M N.
Control strategies for use with magnetic bearings, 4th International Conference on Vibrations in Rotating Machinery, I. Mech. E, September 1988, Edinburgh, Scotland.